Review Article

Lignin ***3***, 9-14 (2022)

The Lignin Society

Lignin

Bacterial Catabolism of a Lignin-derived β–5 Dimer

Naofumi Kamimura, [a,*] and Eiji Masai [a]

[a]*Department of Materials Science and Bioengineering, Nagaoka University of Technology, Nagaoka 940-2188, Japan;*
**Corresponding author: zkami@vos.nagaokaut.ac.jp*

Received: 26 April 2022; revised in form: 24 June 2022; accepted: 25 July 2022

Abstract

The β–5 linkage is an intermolecular linkage in lignin. *Sphingobium* sp. strain SYK-6 can assimilate various lignin-derived dimers, including a β–5 dimer, dehydrodiconiferyl alcohol. In SYK-6, the hydroxyl group at Cγ of the B-ring side chain of dehydrodiconiferyl alcohol is oxidized to generate the γ-carboxylic compound, DCA-C. Then, the hydroxyl group at Cγ of the A-ring side chain of DCA-C is oxidized to the carboxyl group to generate the dicarboxylic compound, DCA-CC. The carboxylic group at Cγ of the A-ring side chain of DCA-CC is decarboxylated, and the accompanying spontaneous ether cleavage of the coumaran ring produces a stilbene-type compound, DCA-S. The conversions of DCA-C and DCA-CC are catalyzed by enantiospecific oxidases (PhcC and PhcD) and enantiospecific decarboxylases (PhcF and PhcG), respectively. DCA-S is subjected to cleavage of the interphenyl double bond by lignostilbene α,β-dioxygenase to generate 5-formylferulate and vanillin. Among the eight lignostilbene α,β-dioxygenase genes, vanillate-induced *lsdD* plays a critical role in cleaving DCA-S. The formyl group of 5-formylferulate is oxidized, and the resultant carboxylic group is subsequently decarboxylated to produce ferulate. Finally, ferulate and vanillin are further catabolized via a previously characterized pathway.

Keywords*: Enantiospecific enzymes; Lignostilbene α,β-dioxygenase; β–5 linkage; Phenylcoumaran; Sphingobium sp. SYK-6*

Lignin, a phenylpropanoid polymer, is a major plant cell wall component and the most abundant aromatic polymer on earth. The microbial degradation of lignin is a critical part of the global carbon cycle, and its catalytic ability is beneficial for lignocellulosic biomass utilization. In lignin, phenylpropane units derived from monolignols are connected via C–C and C–*O*–C linkages [1,2]. In addition to the predominant β–*O*–4 (β-aryl ether) linkage, lignin has β–5 (phenylcoumaran), 5–5 (biphenyl), β–β (resinol), and β–1 (spirodienone) linkages. Microbial degradation of lignin proceeds in two main stages: "depolymerization of native lignin by white-rot fungi," and "mineralization of the resultant aromatic compounds by bacteria." Therefore, elucidating the bacterial catabolism of lignin-derived aromatic compounds is crucial for understanding the final stage of lignin biodegradation in nature.

The β–5 linkage connects two monolignols via C–C and C–*O*–C linkages (Fig. 1) and accounts for 9–12% and 3–11% of the total intermonomer linkages in softwood and hardwood lignin, respectively [3]. Dehydrodiconiferyl alcohol (DCA), a typical β–5 dimer, is one of the major dilignols generated in the initial stages of lignin polymerization [4,5]. Studies of microbial β–5 dimer degradation has mainly been conducted by Japanese researchers. The first report was a 1978 study by Katayama and Fukuzumi [6]. DCA was used as a β–5 dimer, and its degradation pathway by *Pseudomonas putida* FK-2, isolated from an effluent treatment pond in a kraft pulp mill, was partly proposed. After this report, the fungal degradation pathway of DCA was determined in *Fusarium solani* and *Phanerochaete chrysosporium* by Takayoshi Higuchi's research group [7-9]. In 1988, an outline of the bacterial DCA catabolic pathway in *Sphingomonas paucimobilis* TMY1009 was proposed by Habu *et al* [10]. Subsequently, enzymes, thought to be involved in one reaction step of DCA catabolism, were identified and characterized by Kamoda *et al* [11-15]. In recent years, our research group has uncovered a more detailed DCA catabolic pathway, through the analysis of DCA catabolism genes in *Sphingobium* sp. SYK-6 [16-19]. This review

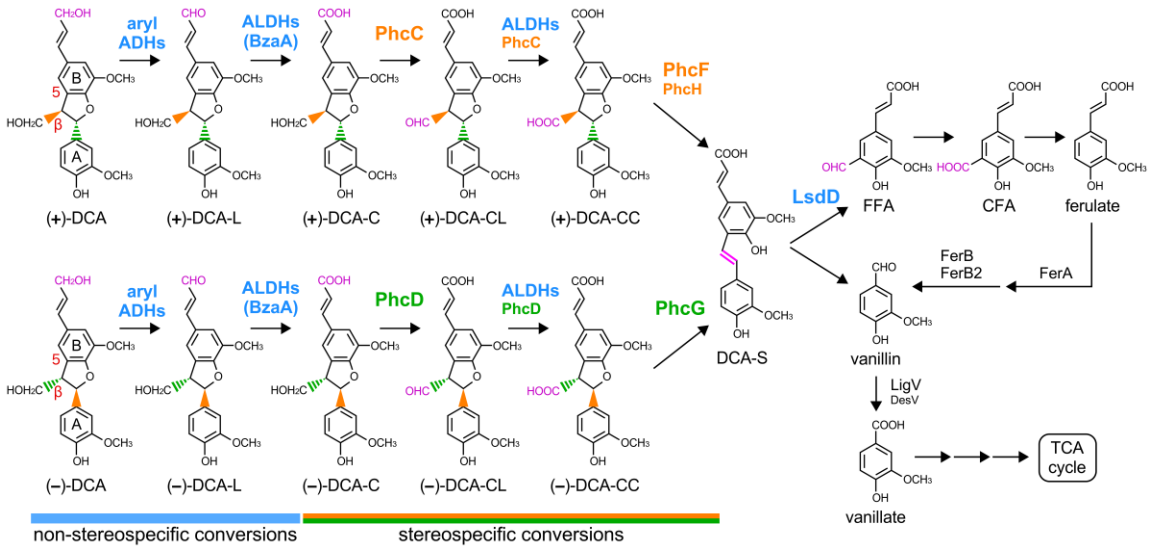

Fig. 1. Catabolic pathway of a β-5 dimer, DCA in *Sphingobium* sp. SYK-6.
Enzymes: ADH, alcohol dehydrogenase; ALDH, aldehyde dehydrogenase; PhcC, (+)-DCA-C oxidase; PhcD, (−)-DCA-C oxidase; PhcF and PhcH, (+)-DCA-CC decarboxylases; PhcG, (−)-DCA-CC decarboxylase; LsdD, lignostilbene α,β-dioxygenase; FerA, feruloyl-coenzyme A (CoA) synthetase; FerB and FerB2, feruloyl-CoA hydratase/lyases; LigV, vanillin dehydrogenase; DesV, syringaldehyde dehydrogenase. Compounds: DCA, dehydrodiconiferyl alcohol; DCA-L, 3-(2-(4-hydroxy-3-methoxyphenyl)-3-(hydroxymethyl)-7-methoxy-2,3-dihydrobenzofuran-5-yl)acrylaldehyde; DCA-C, 3-(2-(4-hydroxy-3-methoxyphenyl)-3-(hydroxymethyl)-7-methoxy-2,3-dihydrobenzofuran-5-yl)acrylate; DCA-CL, 3-(3-formyl-2-(4-hydroxy-3-methoxyphenyl)-7-methoxy-2,3-dihydrobenzofuran-5-yl)acrylate; DCA-CC, 5-(2-carboxyvinyl)-2-(4-hydroxy-3-methoxyphenyl)-7-methoxy-2,3-dihydrobenzofuran-3-carboxylate; DCA-S, 3-(4-hydroxy-3-(4-hydroxy-3-methoxystyryl)-5-methoxyphenyl)acrylate; FFA, 5-formylferulate; CFA, 5-carboxyferulate.

describes advances in our knowledge of bacterial DCA catabolism, which consists of a group of enzymes, including stereospecific oxidases, stereospecific decarboxylases, and side-chain cleavage oxygenases.

Sphingobium sp. SYK-6 is the best-characterized bacterium for catabolism of lignin-derived aromatic compounds [20,21]. This strain catabolizes various lignin-derived dimers, including β-aryl ether, biphenyl, diarylpropane, and phenylcoumaran, as well as monomers, such as ferulate, vanillin, vanillate, syringaldehyde, and syringate. The study of DCA catabolism in SYK-6 was carried out much by the doctoral thesis of our alumnus Kenji Takahashi, who started with pathway determination in 2014 (Fig. 1) [16]. In SYK-6, DCA catabolism is initiated by oxidation of the hydroxyl group at Cγ of the B-ring side chain to produce 3-(2-(4-hydroxy-3-methoxyphenyl)-3-(hydroxymethyl)-7-methoxy-2,3-dihydrobenzofuran-5-yl)acrylate (DCA-C) via the aldehyde derivative, 3-(2-(4-hydroxy-3-methoxyphenyl)-3-(hydroxymethyl)-7-methoxy-2,3-dihydrobenzofuran-5-yl)acrylaldehyde (DCA-L). Thereafter, the hydroxyl group at Cγ of the A-ring side chain of DCA-C is oxidized to generate 5-(2-carboxyvinyl)-2-(4-hydroxy-3-methoxyphenyl)-7-methoxy-2,3-dihydrobenzofuran-3-carboxylate (DCA-CC) via the aldehyde derivative 3-(3-formyl-2-(4-hydroxy-3-methoxyphenyl)-7-methoxy-2,3-dihydrobenzofuran-5-yl)acrylate (DCA-CL). The carboxyl group at Cγ of the A-ring side chain of DCA-CC is further decarboxylated to form a stilbene-type compound, 3-(4-hydroxy-3-(4-hydroxy-3-methoxystyryl)-5-methoxyphenyl)acrylate (DCA-S). The interphenyl Cα–Cβ double bond is then cleaved to generate vanillin and 5-formylferulate from the A- and B-ring portions, respectively. Finally, the formyl group of 5-formylferulate is oxidized, and the resultant carboxyl group is decarboxylated to produce ferulate. This catabolic pathway is fundamentally similar to that suggested in TMY1009. Furthermore, another phenylcoumaran catabolic pathway through 3-methoxy-4-hydroxyphenylglyoxal has been proposed in *Rhodococcus jostii* RHA1 [22].

SYK-6 has at least three and four genes encoding quinohemoprotein alcohol dehydrogenases and aryl alcohol dehydrogenases, respectively, which oxidize DCA to DCA-L [16]. Generally, quinohemoprotein alcohol dehydrogenase uses pyrroloquinoline quinone as the prosthetic group [23], whereas aryl alcohol dehydrogenase requires $NAD(P)^+$ as a coenzyme for the reaction [24]. Since SYK-6 cell extracts require NAD^+ as a coenzyme to oxidize DCA, aryl alcohol dehydrogenases probably play a major role in DCA oxidation. In the next DCA-L oxidation step, aldehyde dehydrogenases (ALDHs) appeared to be involved. SYK-6 has 23 ALDH genes, and multiple ALDH genes are often involved in the oxidation of aromatic aldehydes, such as vanillin, syringaldehyde, vanilloyl acetaldehyde, and syringoyl acetaldehyde [25-27]. Of the 23 ALDH genes, 14 gene products were able to oxidize DCA-L [16]. BzaA showed the highest DCA-L oxidation activity, and disruption of *bzaA* in SYK-6 reduced DCA-L conversion ability. Therefore, while multiple ALDHs are involved in DCA-L oxidation in SYK-6, *bzaA* seems to play a major role in this step.

DCA contains two chiral carbons at the Cα and Cβ positions of the A-ring side chain, and the relative configurations of both carbons are *trans*. Hirai *et al*. determined the absolute configurations of DCA to be (+)-(2*S*,3*R*)-DCA and (–)-(2*R*,3*S*)-DCA (Fig. 1) [28]. In SYK-6, DCA and DCA-L are presumed to be oxidized non-stereospecifically, because the aryl alcohol dehydrogenases and ALDHs, described above, exhibit no stereospecificity (unpublished results). In contrast, DCA-C oxidation and DCA-CC decarboxylation are stereospecific [17,18]. Glucose-methanol-choline (GMC) oxidoreductase family enzymes, PhcC and PhcD, oxidize the hydroxyl group at Cγ of the A-ring side chain of (+)-DCA-C and (–)-DCA-C with strict enantiospecificity, respectively [17]. *phcC* and *phcD* were identified based on the cofactor requirements and transcription induction profiles. Mutant analyses demonstrated that *phcC* and *phcD* are essential for the oxidation of the corresponding DCA-C isomer. Both PhcC and PhcD are localized to the membrane and cytoplasm and can oxidize DCA-C using ubiquinone derivatives, such as CoQ_0 and CoQ_1 as electron acceptors. Therefore, electrons removed from DCA-C by oxidation appeared to be transferred to cytochrome *c* via ubiquinone in vivo. Interestingly, a GMC oxidoreductase family enzyme (HpvZ) is also involved in the oxidation of β-hydroxypropiovanillone, a phenylpropane-type intermediate in β-aryl ether catabolism [27]. Thus, the GMC oxidoreductase family enzymes play important roles in the oxidation of the side chain hydroxyl group at Cγ of some lignin-derived compounds in SYK-6. PhcC and PhcD can oxidize DCA-CL in addition to DCA-C (Fig. 1); however, NAD^+-dependent ALDHs have been suggested to play a significant role in the oxidation of DCA-CL to DCA-CC [17].

PhcF and PhcG catalyze the decarboxylation of the carboxyl group at Cγ of the A-ring side chain of (+)-DCA-CC and (–)-DCA-CC, respectively, to generate DCA-S with strict enantiospecificity (Fig. 1). PhcF and PhcG showed 32% amino acid sequence identity with each other, but there was no significant similarity with known enzymes. Both proteins have a DUF3237 domain with unknown functions. In March 2022, 2546 proteins with the DUF3237 domain are registered (https://pfam.xfam.org/family/PF11578); however, the proteins whose functions have been demonstrated are only PhcF and PhcG, in addition to PhnH, which catalyzes enantioselective hydroalkoxylation of an intermediate of the herqueinone biosynthetic pathway in *Penicillium herquei* [29]. Structural analysis of PhnH showed that this protein forms a β-barrel fold and contains a large central cavity that serves as the putative substrate-binding pocket [30]. Structural comparison of PhnH with some DUF3237 members suggested that these proteins exhibit a similar overall fold. PhcF and PhcG are homotrimers, and their K_m values for DCA-CC were determined to be 84 μM and 103 μM, and V_{max} were 307 $\mu mol \cdot min^{-1} \cdot mg^{-1}$ and 137 $\mu mol \cdot min^{-1} \cdot mg^{-1}$, respectively [18]. In addition to PhcF and PhcG, a nuclear transport factor 2 (NTF2)-like superfamily domain protein, PhcH, exhibits (+)-DCA-CC specific decarboxylation activity (Fig. 1). These genes are localized in tandem and consist of a *phcH-phcG-phcF* operon (unpublished results). Mutant analyses of *phcF*, *phcG*, and *phcH* demonstrated that both *phcF* and *phcG* play major roles in DCA-CC decarboxylation, with a minor contribution from *phcH*. In contrast, the triple mutant of *phcF*, *phcG*, and *phcH* retained a small amount of activity. SYK-6 has six and three homologs of *phcF*/*phcG* and *phcH*, respectively. Among the nine homologs, two *phcF*/*phcG* homologs (SLG_07290 and SLG_28660) and one *phcH* homolog (SLG_30010) exhibited faint activity. These multiple homologs or a different type of decarboxylase may play minor roles in DCA-CC decarboxylation.

An achiral stilbenoid, DCA-S, is formed by the decarboxylation of DCA-CC and cleavage of the α–*O*–4 linkage in the coumaran ring caused by electron transfer from the carboxylate anion associated with decarboxylation. DCA-S is subjected to cleavage of the interphenyl double bond, by lignostilbene α,β-dioxygenase (LSD), to generate 5-formylferulate and vanillin (Fig. 1). Among the eight LSD genes in SYK-6, the gene products of *lsdA*, *lsdC*, *lsdD*, and *lsdG* exhibited DCA-S conversion activity [19]. The DCA-S conversion activity of SYK-6 was induced by vanillate, and the transcription of *lsdA*, *lsdD*, and *lsdG* was induced in the presence of vanillate. Mutant analyses demonstrated that *lsdD* plays a critical role in the conversion of DCA-S during DCA catabolism. In SYK-6, a MarR-type repressor, DesR, which responds to vanillate and syringate, regulates the vanillate and gallate catabolism genes, as well as its own gene [31]. *lsdD* is adjacent upstream of *desR* in the opposite transcription direction. Moreover, the location of the DesR-binding site (IR-R) for *desR* regulation is immediately upstream of the start codon of *lsdD*. These facts suggest that the binding of DesR to IR-R represses transcription of not only *desR*, but also *lsdD*. Recently, Eltis and coworkers revealed the enzymatic and structural features of LsdD of SYK-6 (LSD4 in the nomenclature used by their group) and LsdA of TMY1009 [32,33]. The overall fold of LsdD is a seven-blade β-propeller fold with a cap-like feature on one face formed by extended loops. This structure is common to LsdA of TMY1009 and carotenoid cleavage dioxygenases [32,34]. A catalytic iron(II) ion is bounded to the bipyramidal coordination sphere, distorted by four conserved histidines (His-167, 218, 284, and 476 of LsdD) and a water molecule. The key catalytic residues of LsdD, Phe-59, Tyr-101, and Lys-134 were also conserved. LSDs exhibit a broad substrate range for stilbenoids [19,32], and all SYK-6 LSDs catalyze the cleavage of 1,2-bis(4-hydroxy-3-methoxyphenyl)-1,3-propanediol (HMPPD-S) [19]. HMPPD-S is an intermediate metabolite of a β–1 dimer in TMY1009 [35] and *Novosphingobium aromaticivorans* DSM 12444 [36], and similarly in SYK-6. Among SYK-6 LSDs, LsdH showed the highest oxidizing activity toward HMPPD-S, and its gene transcription level was also the highest during the growth of SYK-6 with vanillate [19]. *lsdH* is likely involved in converting HMPPD-S during β–1 catabolism.

The DCA catabolic pathway has been clarified, and the enzyme genes involved in the steps from DCA oxidation to DCA-S cleavage have been elucidated. Additionally, our research group recently demonstrated the 5-formylferulate catabolic system at the 65th lignin symposium [37]. So, are we close to a complete understanding of the β–5-type dimer catabolic system? It seems there is still quite a long way to go. Firstly, substrate uptake and transcriptional regulation systems are poorly understood. Secondly, we recently discovered that the DCA catabolic pathway is altered in induced and non-induced cells (unpublished results). The pathway presented in this review was determined using cells grown under non-inducing conditions. However, under DCA-inducing conditions, oxidation of the A-ring side chain of DCA, and cleavage of the interphenyl double bond, appear to occur before oxidation of the B-ring side chain of DCA. This observation suggests that the DCA catabolic pathway is altered during culture. Thirdly, DCA, a guaiacyl-type β–5 dimer, is generally used for catabolic studies; however, syringyl- and *p*-hydroxyphenyl-type β–5 dimers also exist [38-40]. In addition, it is not known how the DCA catabolic system of SYK-6 works for the actual β–5 structure-derived compounds produced by lignin biodegradation in nature. Further progress in a more detailed and comprehensive elucidation of the catabolism of β–5 dimers is expected, considering the points mentioned above.

ACKNOWLEDGEMENTS

This work was supported in part by a grant from the Development of Preparatory Basic Bioenergy Technology grant from The New Energy and Industrial Technology Development Organization (NEDO) of Japan, Advanced Low Carbon Technology Research and Development Program from the Japan Science and Technology Agency (Grant No. JPMJAL1107).

REFERENCES

1) Ralph, J. *et al.*, Lignin structure and its engineering, *Curr Opin Biotechnol*, **56**, 240-249 (2019).

2) Vanholme, R. *et al.*, Lignin biosynthesis and structure, *Plant Physiol*, **153**, 895-905 (2010).
3) Zakzeski, J. *et al.*, The catalytic valorization of lignin for the production of renewable chemicals, *Chem Rev*, **110**, 3552-3599 (2010).
4) Tanahashi, M. *et al.*, Dehydrogenative polymerization of 3,5-disubstituted *p*-coumaryl alcohols, *Wood Res*, **61**, 44-53 (1976).
5) Davin, L. B. *et al.*, Stereoselective bimolecular phenoxy radical coupling by an auxiliary (dirigent) protein without an active center, *Science*, **275**, 362-366 (1997).
6) Katayama, Y., Fukuzumi, T., Bacterial degradation of dimers structurally related to lignin. II. Initial intermediate products from dehydrodiconiferyl alcohol by *Pseudomonas putida*, *Mokuzai Gakkaishi*, **24**, 643-649 (1978).
7) Nakatsubo, F. *et al.*, Metabolism of a phenylcoumaran substructure lignin model compound in ligninolytic cultures of *Phanerochaete chrysosporium*, *Arch Microbiol*, **128**, 416-420 (1981).
8) Ohta, M. *et al.*, Microbial degradation of dehydrodiconiferyl alcohol, a lignin substructure model, *Arch Microbiol*, **121**, 23-28 (1979).
9) Umezawa, T. *et al.*, Lignin degradation by *Phanerochaete chrysosporium*: Metabolism of a phenolic phenylcoumaran substructure model compound, *Arch Microbiol*, **131**, 124-128 (1982).
10) Habu, N. *et al.*, Metabolic pathway of dehydrodiconiferyl alcohol by *Pseudomonas* sp. TMY1009, *Mokuzai Gakkaishi*, **34**, 1026-1034 (1988).
11) Kamoda, S. *et al.*, Purification and some properties of lignostilbene-α,β-dioxygenase isozyme IV from *Pseudomonas paucimobilis* TMY1009, *Biosci Biotechnol Biochem*, **61**, 1575-1576 (1997).
12) Kamoda, S., Samejima, M., Cloning of a lignostilbene-α,β-dioxygenase gene from *Pseudomonas paucimobilis* TMY1009, *Agric Biol Chem*, **55**, 1411-1412 (1991).
13) Kamoda, S., Saburi, Y., Structural and enzymatical comparison of lignostilbene-α,β-dioxygenase isozymes, I, II, and III, from *Pseudomonas paucimobilis* TMY1009, *Biosci Biotechnol Biochem*, **57**, 931-934 (1993).
14) Kamoda, S., Saburi, Y., Cloning, expression, and sequence analysis of a lignostilbene-α,β-dioxygenase gene from *Pseudomonas paucimobilis* TMY1009, *Biosci Biotechnol Biochem*, **57**, 926-930 (1993).
15) Kamoda, S. *et al.*, Purification and some properties of lignostilbene-α,β-dioxygenase responsible for the Cα-Cβ cleavage of a diarylpropane type lignin model compound from *Pseudomonas* sp. TMY1009, *Agric Biol Chem*, **53**, 2757-2761 (1989).
16) Takahashi, K. *et al.*, Characterization of the catabolic pathway for a phenylcoumaran-type lignin-derived biaryl in *Sphingobium* sp. strain SYK-6, *Biodegradation*, **25**, 735-745 (2014).
17) Takahashi, K. *et al.*, Membrane-associated glucose-methanol-choline oxidoreductase family enzymes PhcC and PhcD are essential for enantioselective catabolism of dehydrodiconiferyl alcohol, *Appl Environ Microbiol*, **81**, 8022-8036 (2015).
18) Takahashi, K. *et al.*, Two novel decarboxylase genes play a key role in the stereospecific catabolism of dehydrodiconiferyl alcohol in *Sphingobium* sp. strain SYK-6, *Environ Microbiol*, **20**, 1739-1750 (2018).
19) Kamimura, N. *et al.*, LsdD has a critical role in the dehydrodiconiferyl alcohol catabolism among eight lignostilbene α,β-dioxygenase isozymes in *Sphingobium* sp. strain SYK-6, *Int Biodeterior Biodegradation*, **159**, 105208 (2021).
20) Kamimura, N. *et al.*, Bacterial catabolism of lignin-derived aromatics: New findings in a recent decade: Update on bacterial lignin catabolism, *Environ Microbiol Rep*, **9**, 679-705 (2017).
21) Masai, E. *et al.*, Genetic and biochemical investigations on bacterial catabolic pathways for lignin-derived aromatic compounds, *Biosci Biotechnol Biochem*, **71**, 1-15 (2007).
22) Wei, Z. *et al.*, Characterization of thiamine diphosphate-dependent 4-hydroxybenzoylformate decarboxylase enzymes from *Rhodococcus jostii* RHA1 and *Pseudomonas fluorescens* Pf-5 involved in degradation ofaryl C_2 lignin degradation fragments, *Biochemistry*, **58**, 5281-5293 (2019).
23) Toyama, H. *et al.*, Quinohemoprotein alcohol dehydrogenases: structure, function, and physiology, *Arch Biochem Biophys*, **428**, 10-21 (2004).

24) Uthoff, S., Steinbüchel, A., Purification and characterization of an NAD^+-dependent XylB-like aryl alcohol dehydrogenase identified in *Acinetobacter baylyi* ADP1, *Appl Environ Microbiol*, **78**, 8743-8752 (2012).
25) Masai, E. *et al.*, Characterization of *ligV* essential for catabolism of vanillin by *Sphingomonas paucimobilis* SYK-6, *Biosci Biotechnol Biochem*, **71**, 2487-2492 (2007).
26) Kamimura, N. *et al.*, A bacterial aromatic aldehyde dehydrogenase critical for the efficient catabolism of syringaldehyde, *Sci Rep*, **7**, 44422 (2017).
27) Higuchi, Y. *et al.*, Bacterial catabolism of β-hydroxypropiovanillone and β-hydroxypropiosyringone produced in the reductive cleavage of arylglycerol-β-aryl ether in lignin, *Appl Environ Microbiol*, **84** (2018).
28) Hirai, N. *et al.*, Absolute configuration of dehydrodiconiferyl alcohol, *Biosci Biotechnol Biochem*, **58**, 1679-1684 (1994).
29) Gao, S. S. *et al.*, Enzyme-catalyzed intramolecular enantioselective hydroalkoxylation, *J Am Chem Soc*, **139**, 3639-3642 (2017).
30) Feng, Y. *et al.*, Crystal structure and proposed mechanism of an enantioselective hydroalkoxylation enzyme from *Penicillium herquei*, *Biochem Biophys Res Commun*, **516**, 801-805 (2019).
31) Araki, T. *et al.*, Regulation of vanillate and syringate catabolism by a MarR-type transcriptional regulator DesR in *Sphingobium* sp. SYK-6, *Sci Rep*, **9**, 18036 (2019).
32) Kuatsjah, E. *et al.*, Identification of functionally important residues and structural features in a bacterial lignostilbene dioxygenase, *J Biol Chem*, **294**, 12911-12920 (2019).
33) Kuatsjah, E. *et al.*, Structural and functional analysis of lignostilbene dioxygenases from *Sphingobium* sp. SYK-6, *J Biol Chem*, **296**, 100758 (2021).
34) Sui, X. *et al.*, Structural basis of carotenoid cleavage: from bacteria to mammals, *Arch Biochem Biophys*, **539**, 203-213 (2013).
35) Habu, N. *et al.*, Metabolism of a diarylpropane type lignin model compound by *Pseudmonas* sp. TMY1009, *Mokuzai Gakkaishi*, **35**, 348-355 (1989).
36) Presley, G. N. *et al.*, Pathway discovery and engineering for cleavage of a β-1 lignin-derived biaryl compound, *Metab Eng*, **66**, 328-329 (2021).
37) Kawazoe, M. *et al.*, Identification and characterization of the 5-formylferulate catabolism genes in *Sphingobium* sp. SYK-6, *The 65th lignin symposium*, pp. 49-50 (2020).
38) Kuroda, K., Nakagawa-Izumi, A., Tetramethylammonium hydroxide thermochemolysis of guaiacyl-syringyl and guaiacyl dehydrogenation polymers, *Org Geochem*, **36**, 53-61 (2005).
39) Rencoret, J. *et al.*, Structural characterization of milled wood lignins from different eucalypt species, *Holzforschung*, **62**, 514-526 (2008).
40) Wei, X. *et al.*, Deciphering the linkage type and structural characteristics of the *p*-hydroxyphenyl unit in *Pinus massoniana Lamb* compressed wood lignin, *Int J Biol Macromol*, **208**, 772-781 (2022).